

# 1 Mid to late 20<sup>th</sup> century freshening of the western tropical South 2 Atlantic triggered by southward migration of the Intertropical 3 Convergence Zone 4

5 N.S Pereira<sup>1</sup>, L.J. Clarke<sup>2</sup>, C.M. Chiessi<sup>3</sup>, K.H. Kilbourne<sup>4</sup>, S. Crivellari<sup>3</sup>, F.W. Cruz<sup>5</sup>,  
6 J.L.P.S. Campos<sup>5</sup>, T.-L. Yu<sup>6,7</sup>, C.-C. Shen<sup>6,8</sup>, R.K.P. Kikuchi<sup>9</sup>, B.R. Pinheiro<sup>10</sup>, G.O.  
7 Longo<sup>11</sup>, A.N. Sial<sup>12</sup>, T. Felis<sup>13</sup>  
8

9 <sup>1</sup>Department of Exact and Earth Sciences, State University of Bahia, Salvador, Brazil.

10 <sup>2</sup>Department of Natural Sciences, Faculty of Science and Engineering, Manchester  
11 Metropolitan University, Manchester, UK.

12 <sup>3</sup>School of Arts, Sciences and Humanities, University of São Paulo, São Paulo, Brazil,

13 <sup>4</sup>Chesapeake Biological Laboratory, Maryland University, Solomons, US

14 <sup>5</sup>Institute of Geoscience, University of São Paulo, São Paulo, Brazil

15 <sup>6</sup>HISPEC, Department of Geosciences, National Taiwan University., Taipei, Taiwan, ROC.

16 <sup>7</sup>Marine Industry and Engineer Research Center, National Academy of Marine Research,  
17 Koahsiuung, Taiwan, ROC.

18 <sup>8</sup>Research Center for Future Earth, National Taiwan University, Taipei, Taiwan, ROC

19 <sup>9</sup>Department of Oceanography, Federal University of Bahia, Salvador, Brazil.

20 <sup>10</sup>Institute of Biological Sciences and Health, Federal University of Alagoas, Maceió, Brazil.

21 <sup>11</sup>Department of Oceanography and Limnology, Federal University of Rio Grande do Norte,  
22 Natal, Brazil

23 <sup>12</sup>NEG-LABISE, Federal University of Pernambuco, Recife, Brazil.

24 <sup>13</sup>MARUM—Center for Marine Environmental Sciences, University of Bremen, Bremen,  
25 Germany  
26

---

## 27 Abstract

28 In the tropical Atlantic Ocean, the Intertropical Convergence Zone (ITCZ) is an  
29 important climate feature controlled by the interhemispheric sea surface temperature  
30 (SST) gradient, and greatly influences rainfall patterns over the adjacent continents. To  
31 better understand ITCZ dynamics in the context of past and future climate change, long-  
32 term oceanic records are needed, but observational data are limited in temporal extent.  
33 Shallow-water corals provide seasonally-resolved archives of climate variability over  
34 the tropical ocean. Here we present seasonally-resolved records of stable oxygen ( $\delta^{18}\text{O}$ )  
35 and carbon ( $\delta^{13}\text{C}$ ) isotope values of a *Siderastrea stellata* coral from northeastern Brazil  
36 (Maracajaú,  $\sim 5^\circ\text{S}$ ). We show that the long-term trends in the record of coral  $\delta^{18}\text{O}$  values  
37 are not primarily driven by SST but by hydrological changes at the sea surface.  
38 Combining the record of coral  $\delta^{18}\text{O}$  values with instrumental SST, we present the first  
39 reconstruction of seawater  $\delta^{18}\text{O}$  changes ( $\delta^{18}\text{O}_{\text{seawater}}$ ) in the western tropical South  
40 Atlantic back to the early 20<sup>th</sup> century, a parameter that is related to changes in sea  
41 surface salinity. The reconstructed  $\delta^{18}\text{O}_{\text{seawater}}$  changes indicate a prominent freshening  
42 between the mid-1940's and mid-1970's, which coincides with a weakening of the  
43 Atlantic interhemispheric SST gradient during this time interval. Our results suggest  
44 that the weakened Atlantic SST gradient resulted in a southward shift of the thermal  
45 equator that was accompanied by a southward migration of the ITCZ, resulting in  
46 freshening of the western tropical South Atlantic during the mid to late 20<sup>th</sup> century.

47

48 **Keywords:** *Siderastrea stellata*; Coral archive; Stable oxygen isotopes;  
49 Paleoclimatology; ITCZ.

50 **\*Corresponding author: Natan S. Pereira e-mail: nspereira@uneb.br**

---

51

## 52 **1. INTRODUCTION**

53 The Intertropical Convergence Zone (ITCZ) is a well-defined zonally-oriented  
54 band of high precipitation, centered a few degrees to the north of the equator (Schneider  
55 et al. 2014). The ITCZ shows a marked seasonal meridional migration cycle,  
56 characterized by a northernmost position attained during boreal fall and a southernmost  
57 position during boreal spring (Waliser and Gautier 1993). The ITCZ strongly influences  
58 the distribution of rainfall over the tropical Americas, with substantial socio-economic  
59 impacts over northeastern Brazil (Nobre and Shukla 1996; Hastenrath 2012).

60 Observational and modeling studies of the ITCZ indicate that its position is  
61 controlled by the meridional sea-surface temperature (SST) gradient, that changes  
62 seasonally with solar irradiance, as well as oceanic and atmospheric heat transport  
63 (Schneider et al. 2014). However, observational data are extremely limited in temporal  
64 extent and many relevant climatic parameters (e.g., precipitation over the ocean) are  
65 only available after the start of the satellite era. Ocean salinity records from the Atlantic  
66 Ocean, with high enough resolution to resolve the ITCZ, are only available back to the  
67 1970s (Reverdin et al. 2007), although some very sparse data, averaged over large areas  
68 of the ocean, are now available for earlier time periods (Friedman et al. 2017). Land-  
69 based precipitation records can be longer, but few span the whole 20<sup>th</sup> century,  
70 particularly over South America (e.g. Júnior and Lucena 2020). Thus, high temporal  
71 resolution tropical marine paleoclimate records sensitive to ITCZ-related seawater  
72 salinity changes are needed to extend our understanding of ITCZ dynamics.

73 Shallow-water corals can be excellent tropical climate archives (e.g. Weber and  
74 Woodhead 1970; Swart 1983; Swart and Grottooli 2003; Felis 2020). They have been  
75 used to reconstruct oceanographic and climatic changes in the Caribbean Sea (e.g., von  
76 Reumont et al. 2008; Brocas et al. 2016; Fowell et al. 2016), Red Sea (e.g., ; Al-Rousan  
77 et al. 2003; Felis and Rimbu 2010; Murty et al. 2018), Pacific Ocean (e.g., Beck et al.,  
78 1992; Linsley et al. 2010; Carilli et al. 2014) and Indian Ocean (e.g., Gagan et al. 1996;  
79 Lee et al. 2014). Those studies shed light on ocean–climate system phenomena like the  
80 equatorial monsoon (Gagan et al. 1994; Charles et al. 1997; Klein et al. 1997), El Niño  
81 Southern Oscillation (ENSO) (e.g. Fairbanks et al. 1997; Hereid et al. 2012; Cobb et al.  
82 2013; Hetzinger et al. 2016) and the ITCZ (Saenger et al. 2008).

83 In contrast, only a few shallow-water coral records have been generated from  
84 corals sampled in the western tropical South Atlantic (Table 1) (Evangelista et al. 2007,  
85 2018; Mayal et al. 2009; Pereira et al. 2016, 2017, 2018). These studies exclusively  
86 explored two sites (i.e., Rocas atoll and Abrolhos) from all available Brazilian reef  
87 systems (Leão et al. 2016). The few existing coral records from the western tropical  
88 South Atlantic provide valuable information, but do not extend long enough back in  
89 time to facilitate a full understanding of the influence of climate modes and solar  
90 forcing in this understudied region. Among the species with high potential for past  
91 climate reconstruction, the coral species *Siderastrea stellata* is one of the most  
92 important Brazilian reef builders, with a spatial distribution ranging from the equator to  
93 23°S (Lins-de-Barros and Pires 2007). Furthermore, this coral species may provide  
94 geochemical records up to 300 years or more in duration, substantially extending  
95 instrumental climate records from the western tropical South Atlantic.

96

97

98 **Table 1. Coral-based paleoclimate records from the western tropical South Atlantic,**  
 99 **covered period and used paleoclimate proxy.**

Species	Location	Period	Proxy	Reference
<i>Mussismilia braziliensis</i>	Abrolhos reefs	1987 -2003	Sr/Ca, Ba/Ca, Mg/Ca	(Santedicola et al. 2008)
<i>Mussismilia braziliensis</i>	Abrolhos and Tinharé Reef	1998-2005	Growth rate	(Kikuchi et al. 2013)
<i>Siderastrea stellata</i>	Abrolhos	1883-2005	Growth rate	(Evangelista et al. 2015)
<i>Porites astreoides</i>	Rocas atoll	2002-2012	$\delta^{18}\text{O}$ , $\delta^{13}\text{C}$	(Pereira et al. 2015)
<i>Mussismilia leptophylla</i>	Abrolhos	1939–1977	Growth rate	(Evangelista et al. 2007)
<i>Siderastrea stellata</i> , <i>Porites astreoides</i> and <i>Montastrea cavernosa</i>	Rocas atoll	-	$\delta^{53}\text{Cr}$ , $^{87}\text{Sr}/^{86}\text{Sr}$ , $\delta^{13}\text{C}$	(Pereira et al. 2016)
<i>Porites astreoides</i>	Rocas atoll	2001-2013	$\delta^{18}\text{O}$ , $\delta^{13}\text{C}$ , Sr/Ca	(Pereira et al. 2017)
<i>Siderastrea stellata</i>	Rocas atoll	1948-2013	$\delta^{13}\text{C}$	(Pereira et al. 2018)
<i>Siderastrea stellata</i>	Rocas atoll	1970-2009	Sr/Ca, U/Ca	(Evangelista et al. 2018)
<i>Mussismilia hispida</i>	Rocas atoll	1943-1962	$\delta^{18}\text{O}$ , $\delta^{13}\text{C}$	(Silva et al. 2019)
<i>Siderastrea stellata</i>	Maracajaú Reef	1927-2018	$\delta^{18}\text{O}$ , $\delta^{13}\text{C}$	This study

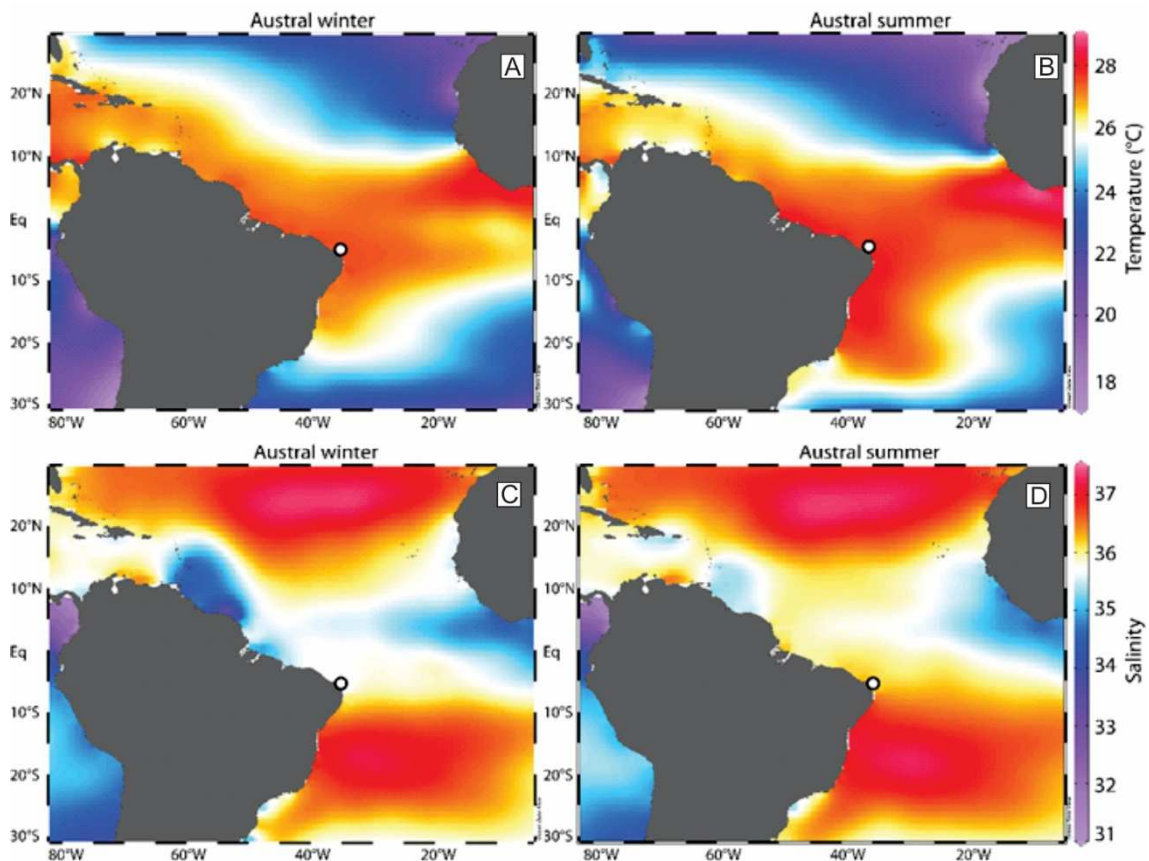
100

101 Here we present records of stable oxygen ( $\delta^{18}\text{O}$ ) and carbon ( $\delta^{13}\text{C}$ ) isotope values  
 102 for a first *Siderastrea Stellata* coral sampled from the Maracajaú reef, situated off  
 103 northeastern Brazil, covering the period from 1929 to 2018. These coral-based stable  
 104 isotope records are by far the longest (i.e., 90-years duration) and highest resolved (i.e.,  
 105 ca. 8 data points per year) datasets from the western tropical South Atlantic. Previous  
 106 work has reported a relatively low performance of the Sr/Ca-temperature proxy in  
 107 tracking SST at interannual and longer timescales off Brazil, when applied to a  
 108 *Siderastrea stellata* coral from Rocas Atoll (Evangelista et al. 2018). Consequently, we  
 109 pair coral  $\delta^{18}\text{O}$  with available instrumental seawater temperatures, in order to provide  
 110 the first reconstruction of the oxygen-isotope composition of seawater ( $\delta^{18}\text{O}_{\text{seawater}}$ ) and  
 111 assess changes in sea surface salinity (SSS), and ITCZ position, in the western tropical

112 South Atlantic throughout the 20<sup>th</sup> Century. We note that application of the Sr/Ca-  
113 temperature proxy to tropical North Atlantic corals of the same genus, *Siderastrea*  
114 *sideria*, has provided more promising results in terms of tracking long-term SST  
115 variability (Maupin 2008; DeLong 2014, 2016; Kuffner 2017; Weerabaddana 2021).

## 116 2. STUDY AREA

117



118

119 **Figure 1. Sea-surface temperature (A and B) and sea-surface salinity (C and D) of the**  
120 **western tropical South Atlantic during austral winter (June-July-August) (A and C) and**  
121 **summer (December-January-February) (B and D). *Siderastrea stellata* coral sampling**  
122 **location at Maracajaú reef is represented by a white circle.**

123

124 This study presents new records of stable carbon and oxygen isotope values for a  
125 *Siderastrea stellata* coral core collected from the shallow coastal reefs of Maracajaú,  
126 these spanning from approximately 5°21'12'' S to 5°25'30'' S and from 35° 14' 30'' W  
127 to 35°17'12'' W, off northeastern Brazil (Fig. 1).

128 The regional climate is tropical, with warm humid conditions and a well-defined  
129 dry season from September to February, contrasting with a wet season from April to  
130 August, with peak precipitation during March–April, when the ITCZ is situated over  
131 northern northeastern Brazil (Chiessi et al. 2021). Wind speed peaks during the wet  
132 season, when SST reaches 26.5°C, and is weaker during the dry season, when seawater  
133 temperature reaches maxima of up to 29.0°C (Testa and Bosence 1999).

134 The Maracajaú reefs are part of an extensive reef complex (~30 km in length from  
135 North to South), situated 5–7 km from the coastline and forming knolls and patch reefs  
136 trending in a northwest–southeast direction, parallel to the coast (Santos et al., 2007).  
137 The study location is situated within the largest coral patch within the Maracajaú reef  
138 complex, this being about 9 km in length and 3 km in width. Water depths in the  
139 complex range from a maximum water depth ca. 5 m to partially exposed patches  
140 during the lowest tides. Scleractinian corals comprise the reef structure, with *S. stellata*  
141 responsible for about 80% of reef construction, alongside calcareous algae (Laborel  
142 1970). The Maracajaú reefs do harbor other scleractinian corals, such as *Porites*  
143 *astreoides*, *Favia gravida*, *Agaricia fragilis* *Agaricia agaricites*, *Porites branneri*,  
144 *Meandrina braziliensis*, *Mussismilia hartii* (Santos et al., 2007) and *Mussismilia hispida*  
145 (rare, Roos et al. 2019), as well as the hydrocorals *Millepora alcicornis*, which form  
146 crowns on the reef tops, and less abundant *Millepora braziliensis* (Santos et al., 2007).

### 147 **3. MATERIAL AND METHODS**

#### 148 **3.1. Sea Surface Temperature**

149 We used SST data from HadISST (Rayner et al. 2003) over the grid point 7° 30'  
150 00'' S and 32° 30' 00'' W, available at the KNMI Climate Explorer  
151 (<https://climexp.knmi.nl>). To evaluate possible differences between different SST data

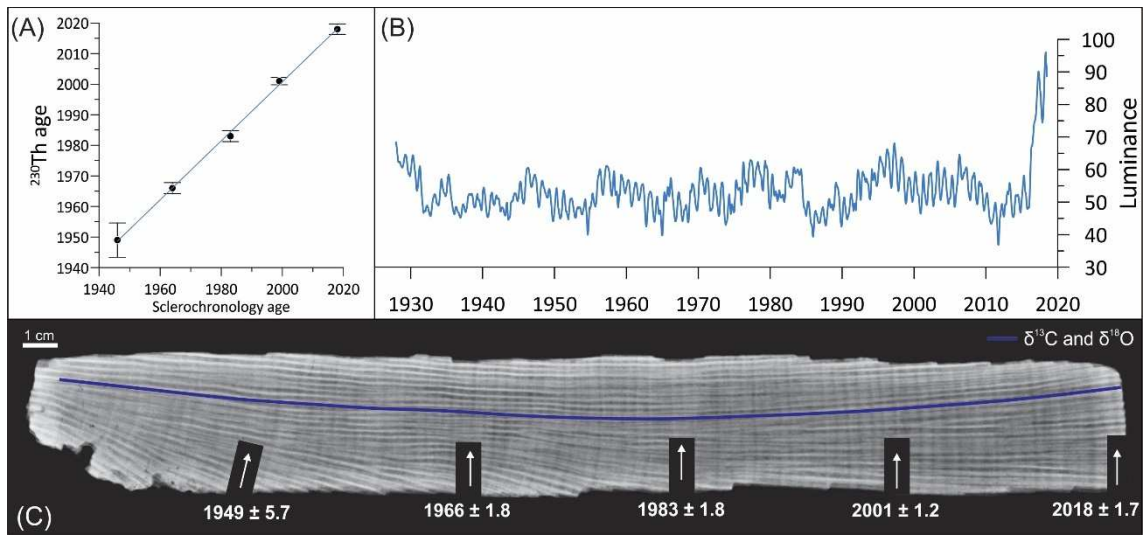
152 products, we also assessed the ERSSTv5 reanalysis data product (Huang et al. 2017),  
153 and the high-resolution satellite Oiv2 SST data products (Reynolds et al. 2002),  
154 obtained from the same coordinates (see supplementary information). The high  
155 correlation between the SST data products indicates that there is no significant  
156 difference between them (Fig. S1) and we decide to use the HadISST data product for  
157 the further analyses developed in this work.

158

### 159 **3.2. Coral sampling**

160 A core of the coral species *Siderastrea stellata* (sample identification number  
161 18SM-C2) was collected from the Maracajaú reef from a water depth ca. 1 m using a  
162 pneumatic drill, retrieving a 34 cm long core. Core 18SM-C2 then was cut into two  
163 halves, with one half cut into 5 mm thick slices, parallel to the growth axis of the whole  
164 *S. stellata* colony. After cutting, the coral slices were cleaned with deionized water, air-  
165 dried and then X-rayed at 50 kV and 320 mA, with an exposure time of 3.2 s and a  
166 distance from equipment to the object of 108 cm.

167 A total of 870 carbonate powder samples were collected by continuous,  
168 progressive milling to 1 mm depth (using a Proxxon micro mill MF 70 coupled with a  
169 precision X-Y table) of the coral slab from the top towards the bottom of the colony,  
170 following the thecal wall, with samples taken in 0.4 mm intervals along the growth axis.  
171 This sampling resolution resulted in about 8 samples per year (using the mean growth  
172 rate as a reference).



174

175 **Figure 2. (A)  $^{230}\text{Th}$  ages versus sclerochronology ages ( $r^2 = 0.99$ ,  $p < 0.0001$ ). (B)**  
 176 **Sclerochronology results from CoralXDS analysis. (C) Coral core 18SM-C2 X-ray image**  
 177 **with sampling track for stable carbon and oxygen isotope analyses (blue line), as well as**  
 178 **sampling locations for  $^{230}\text{Th}$  dating (white arrows).**

179

### 180 3.3. Geochemical analyses

#### 181 3.3.1. $^{230}\text{Th}$ dating

182 Six 0.10–0.25 g subsamples were cut out from along the coral growth axis (Fig. 2)  
 183 for high precision  $^{230}\text{Th}$  dating (Shen et al. 2008, 2012). These subsamples were gently  
 184 crushed, physically cleaned with ultrasonic methods, and dried for U–Th chemistry.  
 185 Chemistry was conducted in a class-10,000 metal-free clean room with class-100  
 186 benches at the High-Precision Mass Spectrometry and Environment Change Laboratory  
 187 (HISPEC), Geosciences Department, National Taiwan University (Shen et al., 2008).  
 188 U–Th isotopic compositions and concentrations were determined on a multi-collector  
 189 inductively-coupled plasma mass spectrometer (MC-ICP-MS) in the HISPEC (Shen et  
 190 al., 2012). The half-lives of U–Th nuclides used for  $^{230}\text{Th}$  age calculation are the given  
 191 half-lives reported in Cheng et al. (2013). Uncertainties in the U–Th isotopic data and  
 192  $^{230}\text{Th}$  dates are calculated at the  $2\sigma$  level (two standard deviations of the mean,  $2\sigma_m$ ),  
 193 unless otherwise noted.



### 194 3.3.2. *Stable-isotope ratio records*

195 Values of  $\delta^{13}\text{C}$  and  $\delta^{18}\text{O}$  of 870 milled coral powder samples were determined at  
196 the Paleoceanography and Paleoclimatology Laboratory, School of Arts, Sciences and  
197 Humanities, University of São Paulo, using a Thermo Scientific™ MAT253 isotope  
198 ratio mass spectrometer coupled to a Thermo Scientific™ Kiel IV automated carbonate  
199 preparation device. Stable isotope measurements were obtained by reaction of 35–100  
200 mg of aragonite with 102% phosphoric acid at 70 °C and the results corrected to permil  
201 units relative to Vienna Pee Dee Belemnite (VPDB) using a calcite-based correction  
202 (Kim et al., 2007). The SHP2L Solnhofen limestone was used as an internal working  
203 standard, which has been calibrated against Vienna Pee Dee Belemnite (VPDB) using  
204 the NBS19 standard (Crivellari et al. 2021). Analytical precision was better than  $\pm 0.05$   
205 ‰ for  $\delta^{13}\text{C}$  and  $\pm 0.07$  ‰ for  $\delta^{18}\text{O}$  ( $\pm 1 \sigma$ ,  $n = 141$ ).

206

### 207 **3.4. Coral core chronology**

208 An age model was developed by counting the density bands using the software  
209 CoralXDS (Helmle et al. 2002) and contrasted to radiometric  $^{230}\text{Th}$  dating (Fig. 2). Then  
210 we compared these results with the number of  $\delta^{18}\text{O}$  cycles, assuming that the  
211 consecutive minima or maxima represent a single year and converted geochemical  
212 records from depth in the coral core to a timescale by pairing highest (and lowest)  $\delta^{18}\text{O}$   
213 with minimum (and maximum) HadiSST data for the region using the software  
214 QanalySeries (Kotov and Pälike 2018).

### 215 **3.5. Seawater $\delta^{18}\text{O}$ reconstruction**

216 Values of  $\delta^{18}\text{O}_{\text{seawater}}$  were deconvoluted from paired coral  $\delta^{18}\text{O}$  and instrumental  
217 SST (HadISST), by adjusting the equation proposed by Cahyarini et al. (2008). To  
218 remove the SST signal from the coral  $\delta^{18}\text{O}$  record and retrieve the  $\delta^{18}\text{O}_{\text{seawater}}$  signal we

219 subtracted the SST contribution, inferred by centered SST, from the centered coral  $\delta^{18}\text{O}$   
220 signal, according to Equation 1 (for more details see Cahyarini et al. 2008 and Pfeiffer  
221 et al. 2019):

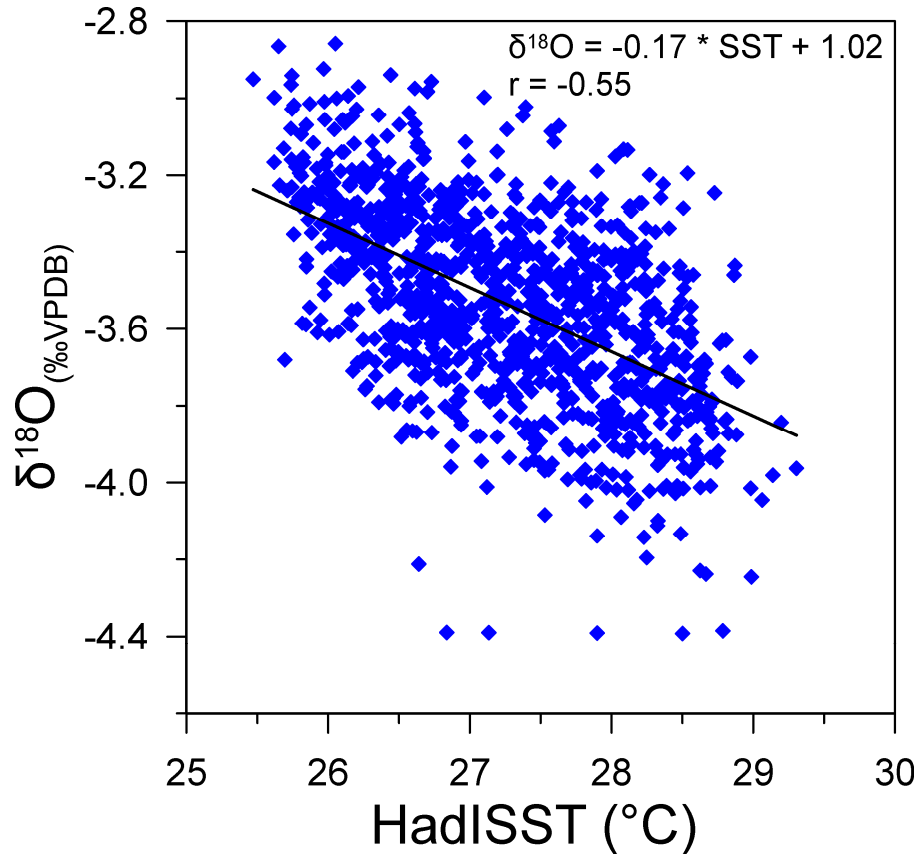
$$222 \text{ Eq (1)} \quad \delta^{18}\text{O}_{\text{seawater}} = (\delta^{18}\text{O}_{\text{coral}} - \overline{\delta^{18}\text{O}_{\text{coral}}}) - (\gamma_1) * (\text{SST} - \overline{\text{SST}})$$

223

224 where  $\delta^{18}\text{O}_{\text{coral}}$  is the measured coral sample,  $\overline{\delta^{18}\text{O}_{\text{coral}}}$  is the mean value of measured  
225  $\delta^{18}\text{O}_{\text{coral}}$  samples, SST is the monthly value obtained from HadISST and equivalent in  
226 time to the  $\delta^{18}\text{O}_{\text{coral}}$  measured on coral,  $\overline{\text{SST}}$  is the mean value of SST over the period  
227 studied.  $\Gamma_1$  is the regression slope of  $\delta^{18}\text{O}_{\text{coral}}$  versus SST retrieved from HadISST.

228 The correlation between  $\delta^{18}\text{O}_{\text{coral}}$  and SST (Fig. 3) yields a  $\delta^{18}\text{O}_{\text{coral}}$ -SST  
229 relationship of  $-0.17\text{‰}$  per  $1^\circ\text{C}$  ( $r = -0.55$ ,  $p < 0.0001$ ), a value slightly higher than the  
230 slope of  $-0.138\text{‰}$  per  $1^\circ\text{C}$  reported by Maupin et al. (2008) for *Siderastrea siderea* in  
231 the Atlantic Ocean, although those authors argue that their slope was likely flatter than  
232 it should have been because of their positive SSS (*i.e.* seawater  $\delta^{18}\text{O}$  contribution) and  
233 SST relationship, which dampens the  $\delta^{18}\text{O}_{\text{coral}}$ -SST relationship. Although the  
234 calibration slope for the Maracajaú *S. stellata* coral is very similar to the well-known  
235 slopes for  $\delta^{18}\text{O}_{\text{coral}}$ -SST in the Indo-Pacific *Porites* corals (e.g., (Gagan et al., 1998;  
236 Omata et al., 2006), the region of Maracajaú is marked by the co-variation of  $\delta^{18}\text{O}_{\text{seawater}}$   
237 and SST, thus the slope obtained by the linear regression between SST and  $\delta^{18}\text{O}$  might  
238 be biased (Cahyarini et al. 2008). In order to evaluate a possible bias, we tested the  
239 influence of different linear regression slopes on the reconstructed  $\delta^{18}\text{O}_{\text{seawater}}$ . Therefore  
240 we compared the  $\delta^{18}\text{O}_{\text{seawater}}$  values obtained based on our linear regression ( $-0.17\text{‰}$   
241 per  $1^\circ\text{C}$ ) to the values obtained based on the linear regressions from Maupin et al.  
242 (2008) ( $-0.138\text{‰}$  per  $1^\circ\text{C}$ ) and Juillet-Leclerc and Schmidt (2001) ( $-0.20\text{‰}$  per  $1^\circ\text{C}$ )  
243 (see supplementary material). We found no substantial difference on the long-term trend

244 of the reconstructed  $\delta^{18}\text{O}_{\text{seawater}}$  when the three different slopes were applied. However,  
 245 we prefer to use the linear regression slope value from the work of Juillet-Leclerc and  
 246 Schmidt (2001) avoiding further issues concerning the influence of seawater isotopic  
 247 composition on the  $\delta^{18}\text{O}_{\text{coral}}$  record and a possible bias generated by the covariation of  
 248 SST and  $\delta^{18}\text{O}_{\text{seawater}}$ .



249  
 250 **Figure 3.**  $\delta^{18}\text{O}$ –SST correlation for coral 18SM-C2 and HadISST (for grid point  $-7.5$   
 251 (latitude) and  $-32.5$  (longitude)). The linear regression of  $\delta^{18}\text{O}$ –SST is significant ( $r =$   
 252  $-0.55$   $p < 0.0001$ ) and the slope is  $-0.17\text{‰}$  per  $1^\circ\text{C}$  (95% CI:  $-0.19, -0.15$ ).

253

### 254 3.5.1. Error propagation

255 The propagated error of reconstructed  $\delta^{18}\text{O}_{\text{seawater}}$  was determined using equation  
 256 (2), modeled after Cahyarini et al., 2008, where  $\sigma_{\delta_{\text{sw}}}$  is the error on reconstructed  
 257  $\delta^{18}\text{O}_{\text{seawater}}$ ,  $\sigma_{\delta_{\text{c}}}$  is the error on measured  $\delta^{18}\text{O}_{\text{coral}}$ ,  $\gamma_1$  is the regression slope of  $\delta^{18}\text{O}_{\text{coral}}$   
 258 versus SST retrieved from HadISST and  $\sigma_{\text{SST}}$  is the error of the HadISST.

259 Eq (2) 
$$\sigma_{\delta_{sw}}^2 = \sigma_{\delta_c}^2 + (\gamma_1)^2 \sigma_{SST}^2$$

260 Combining the analytical error of  $\pm 0.07\text{‰}$  for coral  $\delta^{18}\text{O}$  and HadISST error  
261 varying from 0.10 to 0.76 °C, and the slope value for the  $\delta^{18}\text{O}_{\text{coral}}$ –SST relationship ( $\gamma_1$ )  
262 of  $-0.17\text{‰}$  per 1°C, resulted in an error varying from 0.07 to 0.147 ‰ (Figure 6C), with  
263 a mean error of  $\pm 0.085\text{‰}$  ( $1\sigma$ ) for  $\delta^{18}\text{O}_{\text{seawater}}$ .

264

## 265 **4. RESULTS AND DISCUSSION**

### 266 **4.1. Age model and *S. stellata* coral growth rates**

267 Density-band counting revealed that coral core 18SM-C2 spans the interval from  
268 1928 to 2018. U-Th isotopic compositions and  $^{230}\text{Th}$  dates determined for this coral are  
269 listed in Table 2 and the geochronological approach agrees with density-band counting  
270 (Fig. 2).

271 Excluding the first (1928) and last (2018) years, which might not represent a  
272 complete year of coral growth, the Maracajaú reef *S. stellata* growth rate varied from  
273 2.1 to 5.8 mm year<sup>-1</sup>, with a mean growth rate of  $3.8 \pm 0.7$  mm year<sup>-1</sup> (Fig. 2). The  
274 lowest growth rates were during 1987 (2.1 mm year<sup>-1</sup>), 1937 and 1962 (2.5 mm year<sup>-1</sup>),  
275 1961 (2.5 mm year<sup>-1</sup>), 1938, 1941 and 1986 (2.7 mm year<sup>-1</sup>). The highest growth rates  
276 were during 2012 (5.2 mm year<sup>-1</sup>), 1993 (5.2 mm year<sup>-1</sup>), 1955 (5.4 mm year<sup>-1</sup>), 1959  
277 (5.5 mm year<sup>-1</sup>) and 1944 (5.8 mm year<sup>-1</sup>).

278

279 Table 2. U-Th isotopic compositions and  $^{230}\text{Th}$  ages for subsamples of coral core 18SM-C2.

Analytical errors are  $2\sigma$  of the mean.

Sample ID	Weight g	$^{238}\text{U}$ $10^{-6}\text{g/g}^a$	$^{232}\text{Th}$ $10^{-12}\text{g/g}$	$\delta^{234}\text{U}$ measured <sup>a</sup>	$[\text{}^{230}\text{Th}/\text{}^{238}\text{U}]$ activity <sup>c</sup>	$^{230}\text{Th}/\text{}^{232}\text{Th}$ atomic ( $\times 10^{-6}$ )	Age (yr ago) uncorrected	Age (yr ago) corrected <sup>c,d</sup>	Age (yr BP) relative to 1950 AD	$\delta^{234}\text{U}_{\text{initial}}$ corrected <sup>b</sup>
18SD-1	0.2013	2.3016 ± 0.0020	325.6 ± 2.5	146.0 ± 1.4	0.0000421 ± 0.0000045	4.90 ± 0.53	4.00 ± 0.43	0.7 ± 1.7	-68.8 ± 1.7	146.02 ± 1.4
18SD-2	0.2122	2.3994 ± 0.0023	225.6 ± 2.2	145.4 ± 1.5	0.0002094 ± 0.0000046	36.71 ± 0.89	19.93 ± 0.44	17.8 ± 1.2	-51.8 ± 1.2	145.39 ± 1.5
18SD-3	0.2025	2.0174 ± 0.0017	286.7 ± 2.3	143.0 ± 1.3	0.0004106 ± 0.0000069	47.64 ± 0.89	39.18 ± 0.66	35.9 ± 1.8	-33.8 ± 1.8	143.03 ± 1.3
18SD-4	0.2024	2.2394 ± 0.0019	311.8 ± 2.4	144.0 ± 1.3	0.0005929 ± 0.0000079	70.2 ± 1.1	56.53 ± 0.76	53.3 ± 1.8	-16.2 ± 1.8	144.03 ± 1.3
18SD-5	0.2440	2.3284 ± 0.0028	1113.6 ± 2.4	142.1 ± 1.5	0.000849 ± 0.000015	29.25 ± 0.53	81.0 ± 1.5	70.0 ± 5.7	0.23 ± 5.7	142.17 ± 1.5

<sup>a</sup> $[\text{}^{238}\text{U}] = [\text{}^{235}\text{U}] \times 137.77 (\pm 0.11\%)$  (Hiess et al., 2012);  $\delta^{234}\text{U} = ([\text{}^{234}\text{U}/\text{}^{238}\text{U}]_{\text{activity}} - 1) \times 1000$ .

<sup>b</sup> $\delta^{234}\text{U}_{\text{initial}}$  corrected was calculated based on  $^{230}\text{Th}$  age ( $T$ ), i.e.,  $\delta^{234}\text{U}_{\text{initial}} = \delta^{234}\text{U}_{\text{measured}} \times e^{\lambda^{234}\text{U}T}$ , and  $T$  is corrected age.

<sup>c</sup> $[\text{}^{230}\text{Th}/\text{}^{238}\text{U}]_{\text{activity}} = 1 - e^{-\lambda^{230}\text{Th}T} + (\delta^{234}\text{U}_{\text{measured}}/1000)[\lambda^{230}\text{Th}/(\lambda^{230}\text{Th} - \lambda^{234}\text{U})](1 - e^{-(\lambda^{230}\text{Th} - \lambda^{234}\text{U})T})$ , where  $T$  is the age.

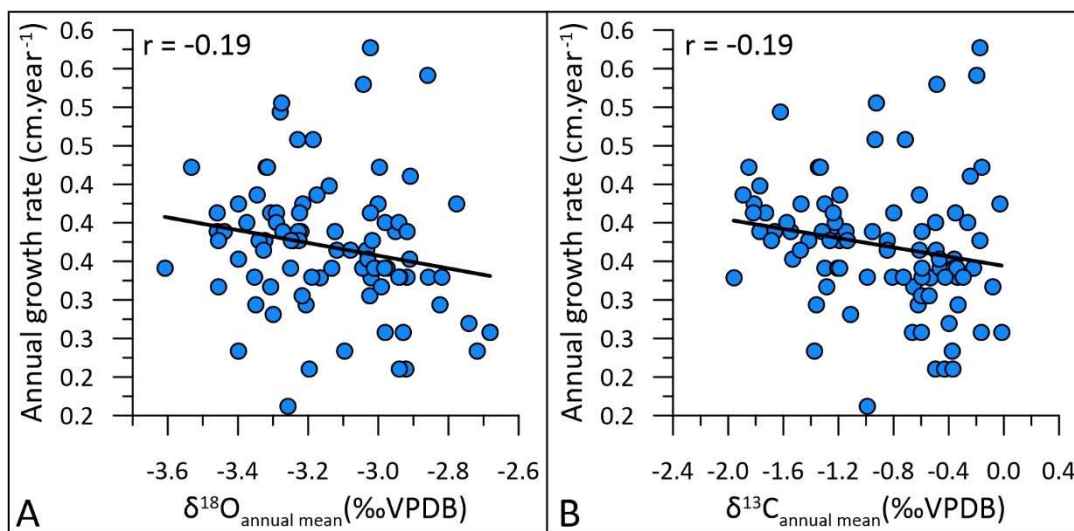
Decay constants are  $9.1705 \times 10^{-6} \text{ yr}^{-1}$  for  $^{230}\text{Th}$ ,  $2.8221 \times 10^{-6} \text{ yr}^{-1}$  for  $^{234}\text{U}$  (Cheng et al., 2013), and  $1.55125 \times 10^{-10} \text{ yr}^{-1}$  for  $^{238}\text{U}$  (Jaffey et al., 1971).

<sup>d</sup>Age corrections, relative to chemistry date on July 15<sup>th</sup> and September 26<sup>th</sup>, 2019, were calculated using an estimated atomic  $^{230}\text{Th}/\text{}^{232}\text{Th}$  ratio of  $4 (\pm 2) \times 10^{-6}$  (Shen et al., 2008).

280

281

282 Before interpretations of the records of  $\delta^{18}\text{O}$  and  $\delta^{13}\text{C}$  values can be made, it is  
 283 important to assess possible growth-rate related kinetic effects (McConnaughey 1989;  
 284 Cohen and McConnaughey 2003), which could compromise coral geochemistry-based  
 285 reconstructions of SST, and ultimately SSS. For the coral *S. stellata* from Maracajaú  
 286 reef, there was no statistically significant relationship between annual growth rates and  
 287 annual mean  $\delta^{18}\text{O}$  and  $\delta^{13}\text{C}$  values ( $p > 0.05$ ; Fig. 4). Consequently, coral core 18SM-C2  
 288  $\delta^{18}\text{O}_{\text{coral}}$  variability seems to be independent of growth rate related kinetic effects  
 289 (McConnaughey 1989; Cohen and McConnaughey 2003).



290  
 291 **Figure 4. Comparison between Maracajaú reef *S. stellata* coral colony 18SM-C2 annual**  
 292 **growth rate and mean annual  $\delta^{18}\text{O}$  ( $p = 0.06$ ) (A); and  $\delta^{13}\text{C}$  ( $p = 0.08$ ) (B) values.**

293

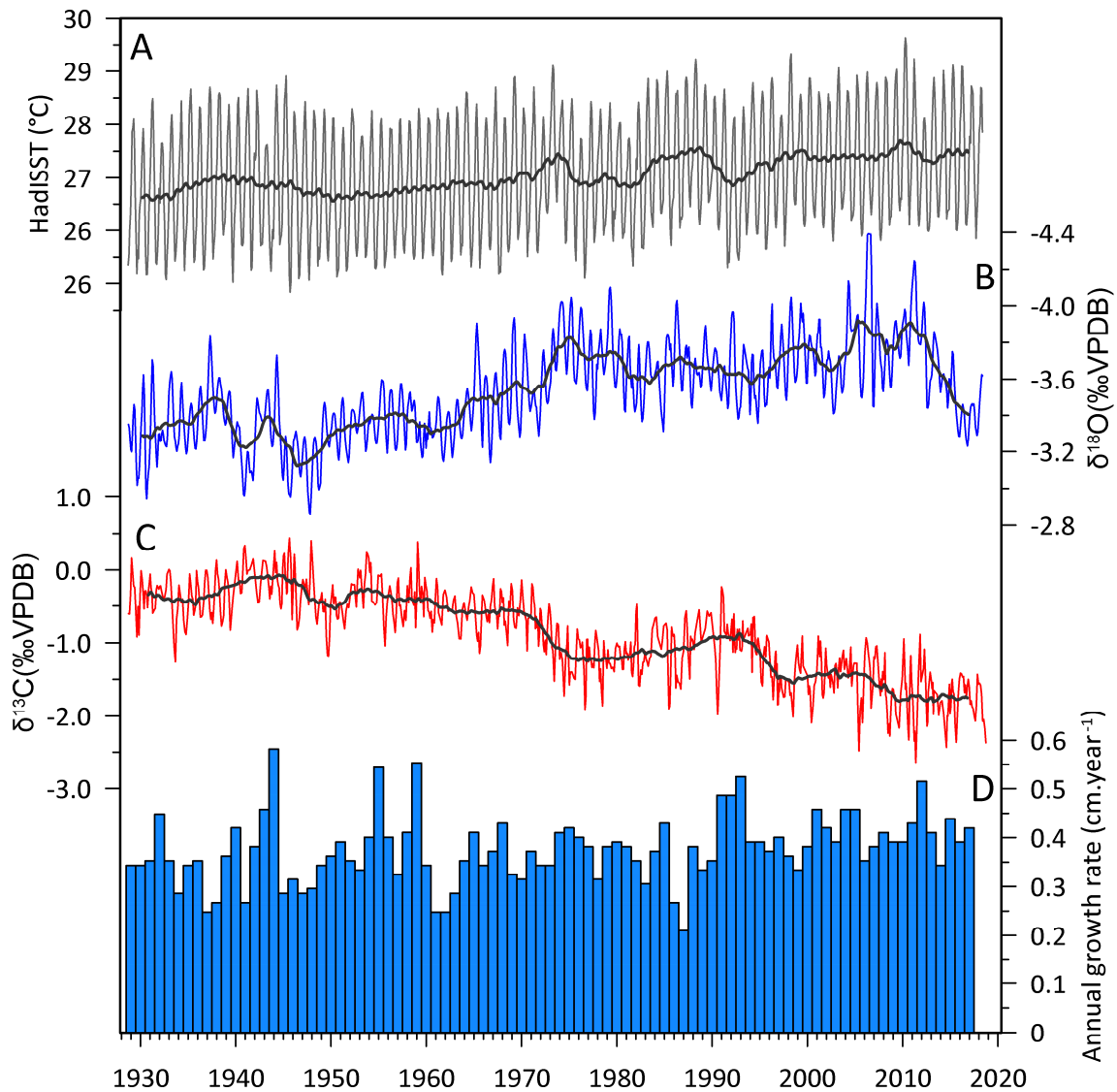
#### 294 4.2. *S. stellata* $\delta^{13}\text{C}$ record

295 Data records of HadISST SST and Maracajaú reef *S. stellata*  $\delta^{13}\text{C}$  and  $\delta^{18}\text{O}$   
 296 records and growth rate are shown in Figure 5.

297 *S. stellata*  $\delta^{13}\text{C}_{\text{coral}}$  values (Fig.5) vary from  $-2.64$  to  $0.44\text{‰}$  and the  $\delta^{13}\text{C}_{\text{coral}}$   
 298 record exhibits short-term (i.e., seasonal or intra-annual) variations, which are usually  
 299 interpreted as a result of seasonal changes in cloud cover and the availability of light.  
 300 Light availability influences coral zooxanthellae symbiont uptake of  $^{12}\text{C}$ , seasonally

301 changing the carbon-isotope composition of the internal dissolved inorganic carbon  
302 pool, from which the coral skeleton is precipitated (Fairbanks and Dodge 1979; Pätzold  
303 1984; Grottoli and Wellington 1999). The  $\delta^{13}\text{C}_{\text{coral}}$  record also shows a general long-  
304 term trend to lower values, after the 1940s. This pattern is consistent with the Suess  
305 Effect (Revelle and Suess 1957; Keeling 1979) which describes the release of  $^{13}\text{C}$ -  
306 depleted  $\text{CO}_2$  into the atmosphere via the burning of fossil fuels, and the subsequent  
307 dissolution of such  $\text{CO}_2$  into the oceans. Similar  $\delta^{13}\text{C}_{\text{coral}}$  trends have been observed in  
308 corals from other Atlantic Ocean sites (Swart et al. 2010) and the Maracajaú reef *S.*  
309 *stellata* decreasing trend of  $-0.019\text{‰}$  per year is consistent with those values reported  
310 by Pereira et al. (2018b) for other Brazilian *Siderastrea* corals sampled from 1948 and  
311 2013 (Table 1).

312



313 1930 1940 1950 1960 1970 1980 1990 2000 2010 2020  
 314 **Figure 5.** A) Sea surface temperatures (SST) for the Maracajaú reef obtained from the  
 315 HadISST product (Kennedy et al. 2019) retrieved from <https://climexp.knmi.nl> for the  
 316 grid point  $-7.5$  (latitude) and  $-32.5$  (longitude). Maracajaú reef *S. stellata* coral core  
 317 18SM-C2  $\delta^{18}\text{O}$  and  $\delta^{13}\text{C}$  time series (B and C, respectively). (D) Coral core 18SM-C2  
 318 annual growth rate. Thick black lines in A-C are running (37-point window) averages.

319

### 320 4.3. *S. stellata* $\delta^{18}\text{O}$ record

321 Gridded instrumental SST for the Maracajaú reef region varied from 25.47 to  
 322 29.30°C, with a mean of  $27.26 \pm 0.84^\circ\text{C}$  and maximum range of 3.83°C, for the period  
 323 from 1928 to 2018 (Fig. 5). The SST time series exhibits an overall general increasing  
 324 trend of  $0.007^\circ\text{C}$  per year, corresponding to an SST increase of  $0.63^\circ\text{C}$  through the 90-  
 325 year study interval.



326 *S. stellata*  $\delta^{18}\text{O}_{\text{coral}}$  varied from  $-4.00$  to  $-2.43\text{‰}$ ; the  $\delta^{18}\text{O}_{\text{coral}}$  record shows clear  
327 lower magnitude seasonal (intra-annual) cycles contrasting with larger magnitude  
328 interannual variability. The complete Maracajaú reef *S. stellata*  $\delta^{18}\text{O}$  record does not  
329 correlate strongly with the independent HadISST SST record for the study region; only  
330 30% of  $\delta^{18}\text{O}$  variance is explained by SST ( $r^2 = 0.30$ ,  $p < 0.001$ ), such that 70% of the  
331  $\delta^{18}\text{O}$  variance must be explained by other forcing variables. Since *S. stellata* growth rate  
332 does not exhibit any strong correlation with  $\delta^{18}\text{O}$  ( $r^2 = 0.04$ ,  $p = 0.06$ ), the next most  
333 plausible explanation is that  $\delta^{18}\text{O}_{\text{coral}}$  variability has been influenced by changing  
334 surface seawater salinity (SSS). Nevertheless, it is important to recognize that, under  
335 specific conditions (e.g. enclosed reef pools),  $\delta^{18}\text{O}_{\text{coral}}$  records may be better recorders  
336 of more localized, reef-scale, SST conditions (Huang et al. 2017; Pfeiffer et al. 2019)  
337 than available wider-scale SST datasets retrieved from combined satellite and in-situ  
338 measurements, the latter also often comprising scarce data measurements that have been  
339 averaged across large spatial scales.

340 An important feature within the  $\delta^{18}\text{O}_{\text{coral}}$  record is an overall decreasing trend, to  
341 lower  $\delta^{18}\text{O}$  values, from the mid-1940s and to the mid-1970s, that is decoupled from the  
342 long-term variability evident in the HadISST SST record. Over this time interval,  
343  $\delta^{18}\text{O}_{\text{coral}}$  has an overall decreasing trend of  $-0.0056\text{‰}$  per year, with a total decrease of  
344  $-0.50\text{‰}$ . Conversion of  $\delta^{18}\text{O}_{\text{coral}}$  into SST (assuming the  $\delta^{18}\text{O}$ -SST relationship of  
345  $0.17\text{‰}/^\circ\text{C}$ ), produces a trend with an annual SST increase of  $0.033^\circ\text{C}$  and a total rise of  
346  $2.96^\circ\text{C}$  for this time interval, more than 4 times the HadISST SST increase for the  
347 region. Even when assuming a ‘traditional’  $\delta^{18}\text{O}$ -SST relationship of  $0.22\text{‰}/^\circ\text{C}$  slope  
348 (Juillet-Leclerc and Schmidt 2001), the observed  $-0.50\text{‰}$  decrease in  $\delta^{18}\text{O}_{\text{coral}}$   
349 represents more than  $2^\circ\text{C}$  increase in SST, indicating that the identified long-term  
350  $\delta^{18}\text{O}_{\text{coral}}$  trend must be influenced by another factor, the most likely one being a change

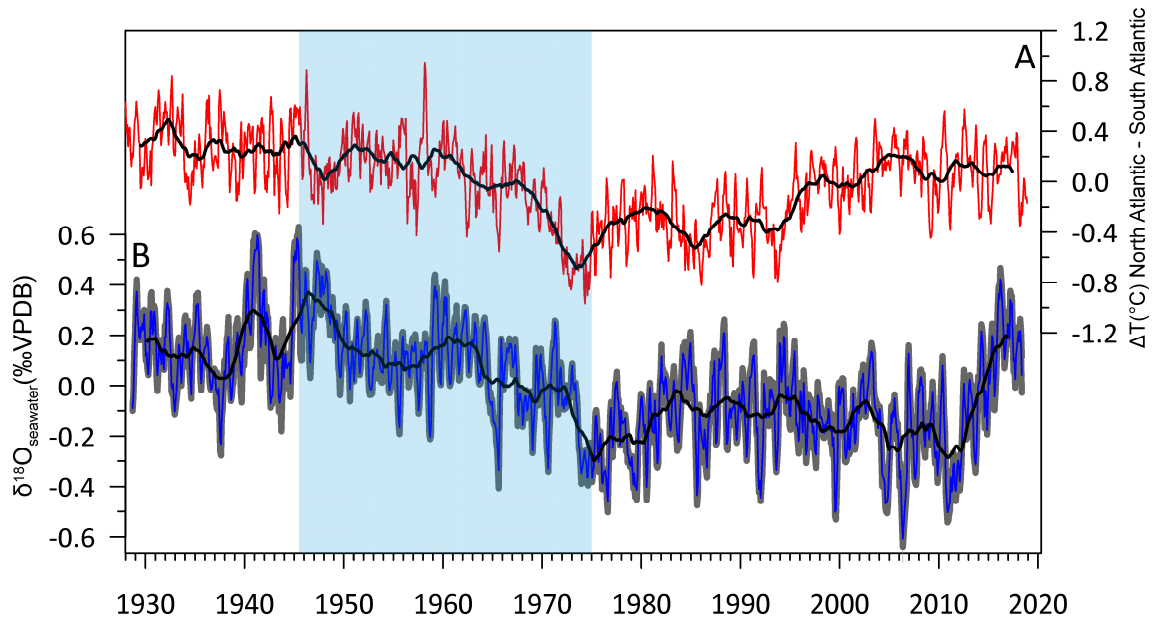
351 in  $\delta^{18}\text{O}_{\text{seawater}}$ . Possible causes of which include the addition of freshwater into the  
352 marine system and/or decreased evaporation from the ocean surface.

353 As detailed above, the largest magnitude Maracajaú reef *S. stellata*  $\delta^{18}\text{O}_{\text{coral}}$   
354 decreasing trend occurs from the mid-1940s to the mid-1970s (Fig. 4), with a  
355 subsequent lower magnitude general decrease between the mid-1970s and ca. 2010. The  
356 change in coral  $\delta^{18}\text{O}$  from 1945 to 1975 is  $-0.55\text{‰}$ , whereas the change in SST over the  
357 same period is  $+0.09^\circ\text{C}$ . Thus, the SST trend can only explain a small fraction of the  
358  $\delta^{18}\text{O}$  change. We suggest that the decreasing trend in coral  $\delta^{18}\text{O}$  from 1945 to 1975 was  
359 caused by a freshening in the upper western tropical South Atlantic.

#### 360 **4.4. $\delta^{18}\text{O}_{\text{seawater}}$ reconstruction**

361 Decoupling the HadISST SST signal from the Maracajaú reef *S. stellata*  $\delta^{18}\text{O}_{\text{coral}}$   
362 record (section 3.3.1) results in a  $\delta^{18}\text{O}_{\text{seawater}}$  reconstruction with a total range of  $1.20\text{‰}$   
363 across the study time interval (Fig. 6). One of the main features of this  $\delta^{18}\text{O}_{\text{seawater}}$   
364 reconstruction is an overall decreasing trend, to more negative  $\delta^{18}\text{O}$  values, from ca.  
365 1947 to ca. 1975. Prior to 1947, average  $\delta^{18}\text{O}_{\text{seawater}}$  values were  $0.17 \pm 0.15\text{‰}$  and  
366 between 1975 and ca. 2012 average  $\delta^{18}\text{O}_{\text{seawater}}$  values were  $-0.16 \pm 0.16\text{‰}$ ; both time  
367 intervals also exhibit some variability in reconstructed  $\delta^{18}\text{O}_{\text{seawater}}$ . After the 1980s, the  
368  $\delta^{18}\text{O}_{\text{seawater}}$  trend stabilized with substantial interannual variations, from ca. 2012,  
369 reconstructed  $\delta^{18}\text{O}_{\text{seawater}}$  increases in magnitude, to more positive values, coincident  
370 with the most intense drought in northeastern Brazil in recent decades (Brito et al.  
371 2018).

372



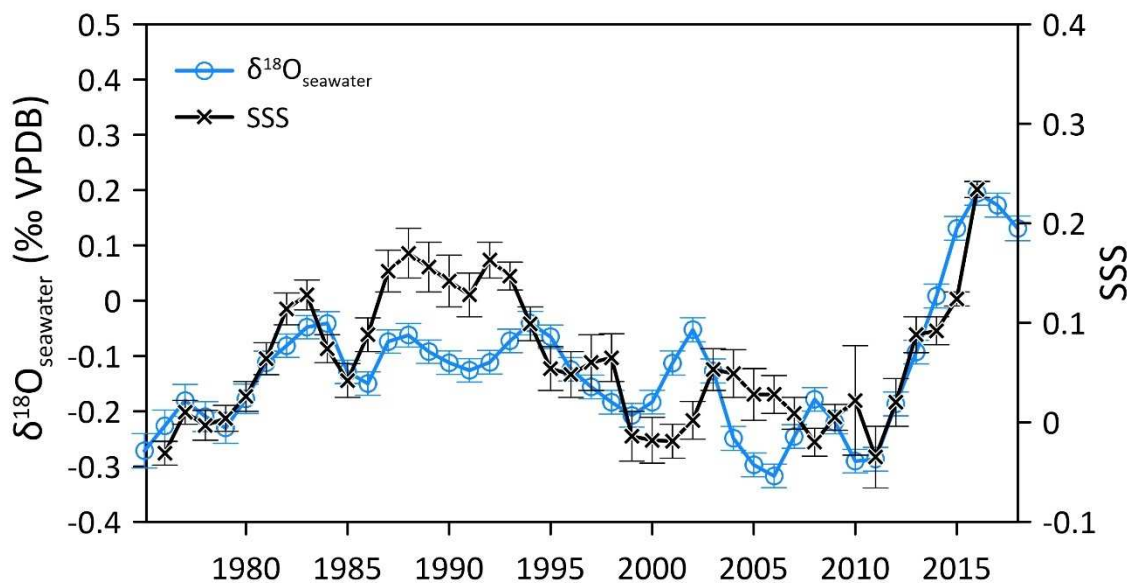
373

374 **Figure 6. (A) Atlantic interhemispheric sea surface temperature (SST) difference from the**  
 375 **HadISST product (Kennedy et al. 2019) (red line) calculated from area-integrated SST of**  
 376 **the North Atlantic (Arctic Circle to equator) and the South Atlantic (Antarctic Circle to**  
 377 **equator) between 68°W and 20°E. The black line is a 37-point running average. (B)**  
 378 **Maracajaú reef seawater  $\delta^{18}\text{O}$  reconstruction (blue line) according to equation (1) with  $\gamma_1$**   
 379 **=  $-0.20\text{‰}/^\circ\text{C}$  (Juillet-Leclerc and Schmidt 2001). Grey shadow is the error propagation**  
 380 **according to equation 2 (separate errors are plotted for each data point), and the black**  
 381 **line is a 37-point running average. A freshening trend (vertical blue shading) is evident**  
 382 **from ca. 1945 to ca. 1975 and coincides with a decrease in the interhemispheric SST**  
 383 **difference between North and South Atlantic (A).**

384

385 Further evidence supporting a robust regional climate signal in our  $\delta^{18}\text{O}_{\text{seawater}}$   
 386 reconstruction can be found in the comparison of our record with a recent SSS data  
 387 compilation (Friedman et al. 2017). When comparing the two datasets for the time  
 388 interval 1975 to 2018, which is a period of abundant instrumental SSS data, the  
 389 Maracajaú reef *S. stellata* coral  $\delta^{18}\text{O}_{\text{seawater}}$  reconstruction is confirmed to be a very good  
 390 proxy for overall trends in regional SSS variability (Fig. 7). Statistical correlations can  
 391 be assessed for two grid boxes included in Friedman et al. (2017); for grid-box 3,  
 392 covering the area 5°N-3°S, 34°W-45°W  $r$  is 0.7 ( $p=0.006$ ,  $N^*=13$ , years 1975-2016),  
 393 and for nearby grid-box 5, spanning 4°N-5°S, 20°W-35°W  $r=0.59$  ( $p=0.03$ ,  $N^*=13$ ,  
 394 years 1975-2016). Before 1975, SSS observations are sparse, during some years

395 observations are absent and values have been interpolated over several years (Friedman  
 396 et al., 2017, supplemental material). Hence, we do not consider SSS correlations to the  
 397 coral-based  $\delta^{18}\text{O}_{\text{seawater}}$  reconstruction prior to 1975 to be a valid exercise. Readers are  
 398 further cautioned that direct calibration between the spatially averaged open-ocean SSS  
 399 data and the single coastal observation from the coral  $\delta^{18}\text{O}$  data is not appropriate  
 400 because of the different amount of averaging inherent in each data source. However, the  
 401 significant amount of shared variance between the datasets demonstrates that the  
 402  $\delta^{18}\text{O}_{\text{seawater}}$  reconstruction based on the Maracajaú reef *S. stellata* coral, which extends  
 403 back to 1928, provides a substantial improvement to existing regional SSS observation.  
 404 In summary, the compelling similarity between the coral-based  $\delta^{18}\text{O}_{\text{seawater}}$   
 405 reconstruction and the instrumental SSS data compilation for this region, during the  
 406 time interval 1975 to 2015 (Friedman et al., 2017), strongly suggests that the coral  
 407 proxy record captures large-scale hydrological signals in the surface ocean of the  
 408 tropical western South Atlantic.



409

410

411 **Figure 7. Instrumental sea surface salinity (SSS) data for the grid-box 5°N-3°S, 34°W-**  
 412 **45°W (Friedman et al., 2017; crosses) and the Maracajaú reef *S. stellata* coral  $\delta^{18}\text{O}_{\text{seawater}}$**   
 413 **reconstruction (circles) demonstrate the sensitivity of the coral  $\delta^{18}\text{O}$  proxy to capture**

414 regional salinity variations. The gridded SSS data are freely available from the French Sea  
415 Surface Salinity Observation Service ([www.legos.obs-mip.fr/observations/sss/](http://www.legos.obs-mip.fr/observations/sss/)). The  
416 salinity data are available as annual March-February means that have been smoothed  
417 with a [121] binomial filter; the  $\delta^{18}\text{O}_{\text{seawater}}$  data have been treated the same to enable  
418 comparison.

419

#### 420 **4.5. Role of the ITCZ in tropical Brazilian Atlantic Ocean change**

421 By examining the  $\delta^{18}\text{O}_{\text{seawater}}$  trend, we observed that most changes to the isotopic  
422 record occurred from 1945 to 1975, with a particularly steep decrease from the mid-  
423 1960s to the mid-1970s (Fig. 6C). The 1945–1975 drop represents a  $\delta^{18}\text{O}_{\text{seawater}}$  change  
424 of  $-0.33\text{‰}$  over a period of ca. 30 years. Using a  $\delta^{18}\text{O}_{\text{seawater}}$ –salinity relationship of  
425  $-0.20 \pm 0.03 \text{‰}$  per psu, as reported by Watanabe et al (2001, 2002) for seawater  
426 collected in the Caribbean Sea, the observed SSS freshening represents a decrease in  
427 SSS of ca. 1.65 psu.

428 The ITCZ position is seasonally regulated by the thermal equator, promoting its  
429 meridional migration throughout the tropics (Schneider et al. 2014). Long-term changes  
430 in the interhemispheric SST gradient would affect the latitudinal displacement of the  
431 ITCZ, shifting its position further north or south according to the SST gradient (Mulitza  
432 et al. 2017; Chiessi et al. 2021), affecting SSS in the western tropical South Atlantic  
433 and, more specifically, in the Maracajaú reef. A southward (northward) migration of the  
434 thermal equator would trigger a decrease (increase) in SSS at the Maracajaú reef.

435 The period from the mid-1940s to the mid-1970s was indeed marked by a  
436 decrease in the SST gradient between the North and the South Atlantic (Fig. 6B). This  
437 change is expected to have shifted the thermal equator to the south, resulting in a  
438 southward migration of the ITCZ and thus in increased precipitation over northern  
439 northeastern Brazil. Such an ITCZ migration is entirely consistent with the  
440 reconstructed  $\delta^{18}\text{O}_{\text{seawater}}$  for the Maracajaú coral reef complex (Fig. 6C). We suggest

441 that the decrease in  $\delta^{18}\text{O}_{\text{seawater}}$  (and SSS) was produced by increased ITCZ-related  
442 precipitation over the Maracajaú reef, western tropical South Atlantic. Furthermore, this  
443 suggestion is consistent with a long-term instrumental precipitation record for Caicó  
444 ( $6^{\circ}27'35''\text{S}$ ;  $37^{\circ}5'56''\text{W}$ ), northeastern Brazil, an inland location about 230 km from  
445 Maracajaú reef, which documents increasing precipitation over the period of 1957 to  
446 1972 (Fig. 6A) (Júnior and Lucena, 2020). Although the exact timing of the SSS  
447 freshening indicated by our Maracajaú reef *S. stellata* coral derived  $\delta^{18}\text{O}_{\text{seawater}}$   
448 reconstruction does not perfectly match the increase in continental precipitation for  
449 Caicó, the instrumental precipitation data clearly supports the notion that a substantial  
450 input of freshwater into northern northeastern Brazil and the western tropical South  
451 Atlantic occurred at least from the late 1950s to the early 1970s as a result of changes in  
452 the interhemispheric Atlantic Ocean temperature gradient.

453         Although our results indicated a freshening in the western South Atlantic Ocean,  
454 instrumental records assessed by Curry et al. (2003) indicated a salinity adjustment at  
455 the Atlantic Ocean, with the tropics becoming more saline between ca. 1950 and 1990.  
456 At the North Atlantic, the observation of Curry et al. (2003) was supported by  
457 Rosenheim et al. (2005) which used sclerosponges records to reconstruct  $\delta^{18}\text{O}_{\text{seawater}}$  of  
458 Salinity Maximum Water from the North Atlantic for the period of 1890-1990, where  
459 they observed a consistent increase in  $\delta^{18}\text{O}_{\text{seawater}}$  from 1950 to 1990. Rosenheim et al  
460 (2005) suggested that the change in salinity is related to recent intensification of the  
461 North Atlantic Oscillation index, which is known to intensify the tradewinds in the  
462 tropical and subtropical North Atlantic (Marshall et al. 2001). Stronger wind stress can  
463 consequently increase evaporation. It might be easy to conclude that these studies are in  
464 contrast to the freshening trend in our data, but they are focused on the broader tropics  
465 and subtropics, not specifically the ITCZ-related SSS minimum region as in our study.

466 An increasing salinity trend over a broad swath of the tropics is consistent with  
467 increased evaporation where  $E > P$ , but the water must go somewhere, and a concomitant  
468 decrease in salinity within the ITCZ-related SSS minimum would indicate that at least  
469 some of it is transported to the deep tropics.

#### 470 **4.6. Connections to the Broader Climate System**

471 The Maracajaú reef *S. stellata* coral derived  $\delta^{18}\text{O}_{\text{seawater}}$  reconstruction is clearly  
472 related to regional SSS (Figure 7), with western tropical South Atlantic SSS linked to  
473 ITCZ-related precipitation (Tchilibou et al., 2015). The SSS changes reconstructed for  
474 the western tropical South Atlantic could represent either a migration of the ITCZ or a  
475 change in the strength of ITCZ-related precipitation, both potentially contributing to the  
476 observed  $\delta^{18}\text{O}_{\text{seawater}}$  signal since 1928. The regional pattern of decreasing SSS in the  
477 western tropical South Atlantic over the last 90 years, with a strong decrease in the  
478 1960s-1970s and a strong recovery in the 2010s, evidenced by our coral record, is  
479 consistent with the broader basin-wide pattern of climate variability over this period.

480 The strong 1960s-1970s SSS decrease shown by the Maracajaú reef *S. stellata*  
481 record is consistent with a southward ITCZ migration, in response to a sharp decrease in  
482 the Atlantic interhemispheric SST gradient (Fig. 6) (Thompson et al. 2010). The timing  
483 of the change coincides with the great salinity anomaly observed in the North Atlantic  
484 Subpolar Gyre (Friedman et al., 2017), and a decrease in Sahel rainfall (Hodson et al.,  
485 2014), that is inverse to the SSS freshening trend off northern northeastern Brazil, all  
486 these observations being consistent with a reduction in AMOC strength (Dima and  
487 Lohmann 2010, Zhang and Delworth 2005). Attempts to explore the causes of the  
488 1960s-1970s interhemispheric temperature shift have ruled out volcanic, ENSO, and  
489 wintertime atmospheric advection forcings (Thompson et al., 2010). Modeling efforts  
490 indicate the change is likely unforced variability and may be related to changes in

491 AMOC, although aerosol forcing cannot be completely discounted (Friedman 2020).  
492 Indeed, AMOC variability is well known to impact ITCZ location across different time  
493 scales (Schneider et al. 2014; Mulitza et al. 2017; Liu et al. 2020), and if this cause is  
494 the major driver of the long-term trend in the Maracajaú reef *S. stellata*  $\delta^{18}\text{O}_{\text{seawater}}$   
495 reconstruction, then our new long-term record would be consistent with recent, though  
496 controversial, claims that the AMOC has slowed down over the 20<sup>th</sup> Century  
497 (Rahmstorf et al., 2015, Caesar et al., 2018, Thornalley et al., 2018, Caesar et al., 2021,  
498 Kilbourne et al., *in press*).

499 The length of the new Maracajaú reef *S. stellata* record also puts the well-  
500 recognized 1960s-1970s shift into a broader context, by showing a long-term decrease  
501 of  $\delta^{18}\text{O}_{\text{seawater}}$  from 1928 to 2010, albeit punctuated by substantial interannual- to  
502 multidecadal-scale variations that culminate with an unprecedented trend to increased  
503 SSS from 2010–2018. This most recent trend and the large reconstructed  $\delta^{18}\text{O}_{\text{seawater}}$   
504 variations during the 1930s-1940s are not associated with a similar change in the  
505 interhemispheric temperature gradient (Fig. 6), unlike the 1960s–1970s shift. This  
506 observation highlights other processes besides the mean location of the ITCZ that can  
507 also influence regional SSS in the western tropical South Atlantic.

508 For instance, the intensity of the Hadley or the Walker Circulation could change  
509 the intensity of ITCZ-related rainfall. Servain et al. (2014) found evidence for  
510 intensification of the Hadley Circulation from 1960-2012. They found no significant  
511 trend in ITCZ location, as calculated by pseudo-windstress curl over those years, but  
512 instead documented warming temperatures centered under the ITCZ and intensification  
513 of the winds, consistent with an intensification of the Hadley cell. The Maracajaú reef *S.*  
514 *stellata* data are consistent with their study, showing no significant trend from



515 1960–2012 because the 1960s–1970s drop in SSS is balanced by the 2010s increase.  
516 Changes in the Walker circulation are thus likely to impact the Maracajaú reef  $\delta^{18}\text{O}$   
517 record. This is not surprising given the strong connection between Atlantic ITCZ-  
518 rainfall, especially during March-April-May, and the Pacific Walker circulation  
519 (Saravanan and Chang 2000, Sasaki et al., 2015). The interaction between the Atlantic  
520 and Pacific can go both ways (McGregor et al., 2014), thus highlighting the potential for  
521 feedbacks between the tropical basins to be impacting the Maracajaú reef *S. stellata*  
522 records.

## 523 5. CONCLUSIONS

524 The first Brazilian *S. stellata* coral  $\delta^{18}\text{O}_{\text{seawater}}$  reconstruction for the Maracajaú  
525 reef complex as presented herewith clearly shows that these corals are promising  
526 archives to understand key western tropical South Atlantic climate features, including  
527 changes in the ITCZ position and the related SSS variability. The new records of  $\delta^{13}\text{C}$   
528 and  $\delta^{18}\text{O}$  values presented here are the longest reconstructions for the western tropical  
529 South Atlantic. The Maracajaú coral  $\delta^{18}\text{O}$  values primarily records SST and the  $\delta^{18}\text{O}$  of  
530 seawater, with no significant growth-related kinetic effects.  $\Delta^{18}\text{O}_{\text{seawater}}$  was  
531 reconstructed by removing the SST contribution to the coral  $\delta^{18}\text{O}$  record using a gridded  
532 instrumental SST product. The reconstructed  $\delta^{18}\text{O}_{\text{seawater}}$  record is marked by a  
533 freshening trend from the 1940s to the 1970s, in agreement with a change in the  
534 interhemispheric temperature gradient during the same period, which also was  
535 coincident with the mid-20<sup>th</sup> Century hiatus in global warming.

536 Since ITCZ location is influenced by the interhemispheric temperature gradient, a  
537 decrease in the SST gradient between the North and the South Atlantic would have  
538 shifted the thermal equator to the south, resulting in southward migration of the ITCZ  
539 and increasing precipitation over northeastern Brazil. Such an ITCZ migration could be

540 related to multidecadal- to centennial-scale variations in AMOC, although definitive  
541 reconstructions of AMOC history are required to test further this relationship. Besides  
542 changes in the latitudinal position of the ITCZ, some of the reconstructed  $\delta^{18}\text{O}_{\text{seawater}}$   
543 variability featured by our Maracajaú reef complex record, could also represent changes  
544 in Hadley and/or Walker cell intensity, which would influence ITCZ-related  
545 precipitation and thus the western tropical South Atlantic SSS. A network of tropical  
546 South Atlantic coral-based SSS records, paired with similar records in the northern  
547 tropics, would facilitate distinguishing between intensity and latitudinal changes in the  
548 ITCZ, thus exploring in greater detail those processes that govern global heat  
549 distribution in the ocean–atmosphere system over decades to centuries, timescales that  
550 are difficult to interrogate with the short-duration instrumental data sets that are  
551 available.

552 In summary, the new Brazilian Maracajaú reef *S. stellata* geochemical records are  
553 an important step towards building a trans-hemispheric network and highlights the  
554 critical importance of tropical South Atlantic coral paleoclimate archives for improving  
555 our understanding of key global climate-system processes.

## 556 **ACKNOWLEDGMENTS**

557 The authors thank two anonymous reviewers as well as the editor for constructive  
558 comments that greatly improved this paper. This study was supported by Serrapilheira  
559 Institute (grant number Serra-1708-15845 to NSP). NSP, CMC, RKPK and GOL also  
560 thank the Brazilian National Council for Scientific and Technology Development  
561 (CNPq) for the research productivity scholarship (grants number 303372/2019-2 to  
562 NSP, 312458/2020-7 to CMC, 311449/2019-0 to RKPK and 310517/2019-2 to GOL).  
563 CMC acknowledges the financial support from FAPESP (grants 2018/15123-4, and  
564 2019/24349-9), CAPES (grant 88881.313535/201901) and the Alexander von

565 Humboldt Foundation. F.W.C and J.L. Campos were funded by FAPESP grant  
566 2017/50085-3. KHK received support from the National Science Foundation grants  
567 OCE 1459636 and OCE 1829385, as well as NOAA Award NA20OAR4310481. This  
568 work represents UMCES contribution number XXXX. Determination of <sup>230</sup>Th ages  
569 was supported by grants from the Science Vanguard Research Program of the  
570 Ministry of Science and Technology (MOST) (110-2123-M-002-009), the  
571 National Taiwan University (109L8926 to C.-C.S.), and the Higher Education  
572 Sprout Project of the Ministry of Education (110L901001 and 110L8907).  
573 NSP and RPKK are members of National Institute of Science and Technology for the  
574 Marine Tropical Environments (INCT AmbTropic grant CNPq 465634/2014-1).

575

## 576 REFERENCES

- 577 Al-Rousan S, Al-Moghrabi S, Pätzold J, Wefer G (2003) Stable oxygen isotopes in  
578 Porites corals monitor weekly temperature variations in the northern Gulf of  
579 Aqaba, Red Sea. *Coral Reefs* 22:346–356
- 580 Beck JW, Edwards RL, Ito E, Taylor FW, Recy J, Rougerie F, Joannot P, Henin C  
581 (1992) Sea-surface temperature from coral skeletal strontium/calcium ratios.  
582 *Science* 257:644–7
- 583 Brito SSB, Cunha APMA, Cunningham CC, Alvalá RC, Marengo JA, Carvalho MA  
584 (2018) Frequency, duration and severity of drought in the Semiarid Northeast  
585 Brazil region. *Int J Climatol* 38:517–529
- 586 Brocas WM, Felis T, Obert JC, Gierz P, Lohmann G, Scholz D, Kölling M, Scheffers  
587 SR (2016) Last interglacial temperature seasonality reconstructed from tropical  
588 Atlantic corals. *Earth Planet Sci Lett* 449:418–429
- 589 Cahyarini SY, Pfeiffer M, Timm O, Dullo WC, Schönberg DG (2008) Reconstructing  
590 seawater  $\delta^{18}\text{O}$  from paired coral  $\delta^{18}\text{O}$  and Sr/Ca ratios: Methods, error analysis  
591 and problems, with examples from Tahiti (French Polynesia) and Timor  
592 (Indonesia). *Geochim Cosmochim Acta* 72:2841–2853
- 593 Carilli JE, McGregor H V., Gaudry JJ, Donner SD, Gagan MK, Stevenson S, Wong H,  
594 Fink D (2014) Equatorial Pacific coral geochemical records show recent  
595 weakening of the Walker Circulation. *Paleoceanography* 29:1031–1045
- 596 Charles CD, Hunter D., Fairbanks RG (1997) REPORTS m a Interaction Between the

- 597 ENSO and the Asian Monsoon in a Coral Record of Tropical Climate. *Science* (80-  
598 ) 277:925–928
- 599 Cheng H, Edwards RL, Shen C-C, Polyak VJ, Asmerom Y, Woodhead J, Hellstrom J,  
600 Wang Y, Kong X, Spötl C, Wang X, Alexander EC (2013) Improvements in  $^{230}\text{Th}$   
601 dating,  $^{230}\text{Th}$  and  $^{234}\text{U}$  half-life values, and U–Th isotopic measurements by multi-  
602 collector inductively coupled plasma mass spectrometry. *Earth Planet Sci Lett*  
603 371–372:82–91
- 604 Chiessi CM, Mulitza S, Taniguchi NK, Prange M, Campos MC, Häggi C, Schefuß E,  
605 Pinho TML, Frederichs T, Portilho-Ramos RC, Sousa SHM, Crivellari S, Cruz FW  
606 (2021) Mid- to Late Holocene Contraction of the Intertropical Convergence Zone  
607 Over Northeastern South America. *Paleoceanogr Paleoclimatology*  
608 36:e2020PA003936
- 609 Cobb KM, Westphal N, Sayani HR, Watson JT, Di Lorenzo E, Cheng H, Edwards RL,  
610 Charles CD (2013) Highly variable El Niño–Southern Oscillation throughout the  
611 Holocene. *Science* 339:67–70
- 612 Cohen AL, McConnaughey TA (2003) Geochemical Perspectives on Coral  
613 Mineralization.
- 614 Crivellari S, Viana PJ, Campos MDC, Kuhnert H, Machado Lopes AB, Cruz FW Da,  
615 Chiessi CM (2021) Development and characterization of a new in-house reference  
616 material for stable carbon and oxygen isotopes analyses. *J Anal At Spectrom*  
617 36:1125–1134
- 618 Curry R, Dickson B, Yashayaev I (2003) A change in the freshwater balance of the  
619 Atlantic Ocean over the past four decades. *Nature* 426:826–829
- 620 DeLong KL, Maupin CR, Flannery JA, Quinn TM, Shen C-C (2016) Refining  
621 temperature reconstructions with the Atlantic coral *Siderastrea siderea*.  
622 *Palaeogeogr Palaeoclimatol Palaeoecol*
- 623 DeLong KL, Quinn TM, Taylor FW, Shen C-C, Lin K (2013) Improving coral-base  
624 paleoclimate reconstructions by replicating 350 years of coral Sr/Ca variations.  
625 *Palaeogeogr Palaeoclimatol Palaeoecol* 373:6–24
- 626 Felis T (2020) Extending the instrumental record of ocean-atmosphere variability into  
627 the last interglacial using tropical corals. *Oceanography* 33:69–79
- 628 Huang B, Thorne PW, Banzon VF, Boyer T, Chepurin G, Lawrimore JH, Menne MJ,  
629 Smith TM, Vose RS, Zhang HM (2017) Extended reconstructed Sea surface  
630 temperature, Version 5 (ERSSTv5): Upgrades, validations, and intercomparisons. *J*  
631 *Clim* 30:8179–8205
- 632 Juillet-Leclerc A, Schmidt G (2001) A calibration of the oxygen isotope  
633 paleothermometer of coral aragonite from *Porites*. *Geophys Res Lett* 28:4135–  
634 4138
- 635 Kuffner IB, Roberts KE, Flannery JA, Morrison JM, Richey JN (2017) Fidelity of the  
636 Sr/Ca proxy in recording ocean temperature in the western Atlantic coral  
637 *Siderastrea siderea*. *Geochemistry, Geophys Geosystems* 18:178–188
- 638 Marshall J, Kushnir Y, Battisti D, Chang P, Czaja A, Dickson R, Hurrell J, McCartney  
639 M, Saravanan R, Visbeck M (2001) North Atlantic climate variability: Phenomena,

640 impacts and mechanisms. *Int J Climatol* 21:1863–1898

641 Rayner NA, Parker DE, Horton EB, Folland CK, Alexander L V, Rowell DP, Kent EC,  
642 Kaplan A (2003) Global analyses of sea surface temperature, sea ice, and night  
643 marine air temperature since the late nineteenth century. *J Geophys Res* 108:4407

644 Reynolds RW, Rayner NA, Smith TM, Stokes DC, Wang W (2002) An improved in  
645 situ and satellite SST analysis for climate. *J Clim* 15:1609–1625

646 Rosenheim BE, Swart PK, Thorrold SR, Eisenhauer A, Willenz P (2005) Salinity  
647 change in the subtropical Atlantic: Secular increase and teleconnections to the  
648 North Atlantic Oscillation. *Geophys Res Lett* 32:1–4

649 SWART PK (1983) Carbon and Oxygen Isotope Fractionation in Scleractinian Corals: a  
650 Review. *Earth-Science Rev* 19:51–80

651 Swart PK, Grottoli a. (2003) Proxy indicators of climate in coral skeletons: a  
652 perspective. *Coral Reefs* 22:313–315

653 Weber J, Woodhead P (1970) Carbon and oxygen isotope fractionation in the skeletal  
654 carbonate of reef-building corals. *Chem Geol* 6:93–117

655 Evangelista H, Godiva D, Sifeddine A, Leão ZM a. N, Rigozo NR, Segal B, Ambrizzi  
656 T, Kampel M, Kikuchi RKP, Le Cornec F (2007) Evidences linking ENSO and  
657 coral growth in the Southwestern-South Atlantic. *Clim Dyn* 29:869–880

658 Evangelista H, Sifeddine A, Corrège T, Servain J, Dassié EP, Logato R, Cordeiro RC,  
659 Shen C-C, Le Cornec F, Nogueira J, Segal B, Castagna A, Turcq B (2018)  
660 Climatic Constraints on Growth Rate and Geochemistry (Sr/Ca and U/Ca) of the  
661 Coral *Siderastrea stellata* in the Southwest Equatorial Atlantic (Rocas Atoll,  
662 Brazil). *Geochemistry, Geophys Geosystems* 19:772–786

663 Evangelista H, Wainer I, Sifeddine A, Corrège T, Cordeiro RC, Lamounier S, Godiva  
664 D, Shen C-C, Le Cornec F, Turcq B, Lazareth CE, Hu C-Y (2015) Southwestern  
665 Tropical Atlantic coral growth response to atmospheric circulation changes  
666 induced by ozone depletion in Antarctica. *Biogeosciences Discuss* 12:13193–  
667 13213

668 Fairbanks RG, Dodge RE (1979) Annual periodicity of the the 18O/16O and 13C/12C  
669 and ratios in the coral *Montastrea annularis*. *Geochim Cosmochim Acta* 43:1009–  
670 1020

671 Fairbanks RG, Evans MN, Rubenstone JL, Mortlock RA, Broad K, Moore MD, Charles  
672 CD (1997) Evaluating climate indices and their geochemical proxies found in  
673 corals. *Coral Reefs* 16:S93–S100

674 Felis T (2020) Extending the instrumental record of ocean-atmosphere variability into  
675 the last interglacial using tropical corals. *Oceanography* 33:69–79

676 Felis T, Pätzold J, Loya Y (2003) Mean oxygen-isotope signatures in *Porites* spp.  
677 Corals: inter-colony variability and correction for extension-rate effects. *Coral*  
678 *Reefs* 22:328–336

679 Felis T, Pätzold J, Loya Y, Fine M, Nawar AH, Wefer G (2000) A coral oxygen isotope  
680 record from the northern Red Sea documenting NAO, ENSO, and North Pacific  
681 teleconnections on Middle East climate variability since the year 1750.

- 682 Paleocyanography 15:679–694
- 683 Felis T, Rimbu N (2010) Mediterranean climate variability documented in oxygen  
684 isotope records from northern Red Sea corals—A review. *Glob Planet Change*  
685 71:232–241
- 686 Fowell SE, Sandford K, Stewart JA, Castillo KD, Ries JB, Foster GL (2016) Intra-reef  
687 variations in Li/Mg and Sr/Ca sea surface temperature proxies in the Caribbean  
688 reef-building coral *Siderastrea siderea*. *Paleocyanography* 1315–1329
- 689 Friedman AR, Reverdin G, Khodri M, Gastineau G (2017) A new record of Atlantic sea  
690 surface salinity from 1896 to 2013 reveals the signatures of climate variability and  
691 long-term trends. *Geophys Res Lett* 44:1866–1876
- 692 Gagan MK, Ayliffe LK, Hopley D, Cali JA, Mortimer GE, Chappell J, Mcculloch MT,  
693 Head MJ (1998) Temperature and surface-ocean water balance of the mid-  
694 holocene tropical western pacific. *Science* 279:1014–8
- 695 Gagan MK, Chivas AR, Isdale PJ (1994) High-resolution isotopic records from corals  
696 using ocean temperature and mass-spawning chronometers. *Earth Planet Sci Lett*  
697 121:549–558
- 698 Gagan MK, Chivas AR, Isdale PJ (1996) Timing coral-based climatic histories using  
699  $^{13}\text{C}$  enrichments driven by synchronized spawning. *Geology* 24:1009–1012
- 700 Grottoli a. G, Wellington GM (1999) Effect of light and zooplankton on skeletal  $\delta^{13}\text{C}$   
701 values in the eastern Pacific corals *Pavona clavus* and *Pavona gigantea*. *Coral*  
702 *Reefs* 18:29–41
- 703 Hathorne EC, Felis T, Suzuki A, Kawahata H, Cabioch G (2013) Lithium in the  
704 aragonite skeletons of massive *Porites* corals: A new tool to reconstruct tropical  
705 sea surface temperatures. *Paleocyanography* 28:
- 706 Hereid KA, Quinn TM, Taylor FW, Shen C-C, Lawrence Edwards R, Cheng H (2012)  
707 Coral record of reduced El Nino activity in the early 15<sup>th</sup> to middle 17<sup>th</sup> centuries.  
708 *Geology* 41:51–54
- 709 Hetzinger S, Pfeiffer M, Dullo W-C, Zinke J, Garbe-Schönberg D (2016) A change in  
710 coral extension rates and stable isotopes after El Niño-induced coral bleaching and  
711 regional stress events. *Sci Rep* 6:32879
- 712 Hiess J., Condon DJ., McLean N. and Noble SR. (2012)  $^{238}\text{U}/^{235}\text{U}$  systematics in  
713 terrestrial uranium-bearing minerals. *Science* 355, 1610-1614.
- 714 Huang B, Thorne PW, Banzon VF, Boyer T, Chepurin G, Lawrimore JH, Menne MJ,  
715 Smith TM, Vose RS, Zhang HM (2017) Extended reconstructed Sea surface  
716 temperature, Version 5 (ERSSTv5): Upgrades, validations, and intercomparisons. *J*  
717 *Clim* 30:8179–8205
- 718 Jaffey AH, Flynn KF, Glendenin LE, Bentley WC and Essling AM. (1971) Precision  
719 measurement of half-lives and specific activities of  $^{235}\text{U}$  and  $^{238}\text{U}$ . *Phys. Rev. C* 4,  
720 1889–1906.
- 721 Juillet-Leclerc A, Schmidt G (2001) A calibration of the oxygen isotope  
722 paleothermometer of coral aragonite from *Porites*. *Geophys Res Lett* 28:4135–  
723 4138

- 724 Júnior JBC, Lucena RL (2020) Analysis of Precipitation Using Mann-Kendall and  
725 Kruskal-Wallis Non-Parametric Tests. *Mercator* 19:1–14
- 726 Keeling CD (1979) The Suess effect: <sup>13</sup>Carbon-<sup>14</sup>Carbon interrelations. *Environ Int*  
727 2:229–300
- 728 Kennedy JJ, Rayner NA, Atkinson CP, Killick RE (2019) An Ensemble Data Set of Sea  
729 Surface Temperature Change From 1850: The Met Office Hadley Centre  
730 HadSST.4.0.0.0 Data Set. *J Geophys Res Atmos* 124:7719–7763
- 731 Kikuchi RKP, Oliveira MDM, Leão ZMAN (2013) Density banding pattern of the south  
732 western Atlantic coral *Mussismilia braziliensis*. *J Exp Mar Bio Ecol* 449:207–214
- 733 Klein R, Tudhope AW, Chilcott CP, Pätzold J, Abdulkarim Z, Fine M, Fallick AE,  
734 Loya Y (1997) Evaluating southern Red Sea corals as a proxy record for the Asian  
735 monsoon. *Earth Planet Sci Lett* 148:381–394
- 736 Knutson TR, Zhang R, Horowitz LW (2016) Prospects for a prolonged slowdown in  
737 global warming in the early 21<sup>st</sup> century. *Nat Commun* 7:1–12
- 738 Kotov S, Pälke H (2018) QanalySeries – a cross-platform time series tuning and  
739 analysis tool.
- 740 Laborel J (1970) Les peuplements de madréporaires des cotes tropicales du Brésil. *Ann*  
741 *L'Université D'Abidjan* 2: 260
- 742 Leão ZMAN, Kikuchi RKP, Ferreira BP, Neves EG, Sovierzoski HH, Oliveira MDM,  
743 Maida M, Correia MD, Johnsson R (2016) Brazilian coral reefs in a period of  
744 global change: A synthesis. *Brazilian J Oceanogr* 64:97–116
- 745 Lee J, Boyle EA, Suci I, Pfeiffer M, Meltzner AJ, Suwargadi B (2014) Coral-based  
746 history of lead and lead isotopes of the surface Indian Ocean since the mid-20<sup>th</sup>  
747 century. *Earth Planet Sci Lett* 398:37–47
- 748 Lins-de-Barros M, Pires DO (2007) COMPARISON OF THE REPRODUCTIVE  
749 STATUS OF THE SCLERACTINIAN CORAL *SIDERASTREA STELLATA*  
750 THROUGHOUT A GRADIENT OF 20° OF LATITUDE. *Brazilian J Oceanogr*  
751 55:67–69
- 752 Linsley BK, Rosenthal Y, Oppo DW (2010) Holocene evolution of the Indonesian  
753 throughflow and the western Pacific warm pool. *Nat Geosci* 3:578–583
- 754 Liu W, Fedorov A V., Xie SP, Hu S (2020) Climate impacts of a weakened Atlantic  
755 meridional overturning circulation in a warming climate. *Sci Adv* 6:eaz4876
- 756 Maupin CR, Quinn TM, Halley RB (2008) Extracting a climate signal from the skeletal  
757 geochemistry of the Caribbean coral *Siderastrea siderea*. *Geochemistry, Geophys*  
758 *Geosystems* 9:n/a-n/a
- 759 Mayal EM, Sial AN, Ferreira VP, Fisner M, Pinheiro BR (2009) Thermal stress  
760 assessment using carbon and oxygen isotopes from *Scleractinia*, Rocas Atoll,  
761 northeastern Brazil. *51:166–188*
- 762 McConnaughey T (1989) <sup>13</sup>C and <sup>18</sup>O isotopic disequilibrium in biological carbonates :  
763 I. Patterns. *53:151–162*
- 764 Mulitza S, Chiessi CM, Schefuß E, Lippold J, Wichmann D, Antz B, Mackensen A,

- 765 Paul A, Prange M, Rehfeld K, Werner M, Bickert T, Frank N, Kuhnert H, Lynch-  
766 Stieglitz J, Portilho-Ramos RC, Sawakuchi AO, Schulz M, Schwenk T, Tiedemann  
767 R, Vahlenkamp M, Zhang Y (2017) Synchronous and proportional deglacial  
768 changes in Atlantic meridional overturning and northeast Brazilian precipitation.  
769 *Paleoceanography* 32:622–633
- 770 Murty SA, Bernstein WN, Ossolinski JE, Davis RS, Goodkin NF, Hughen KA (2018)  
771 Spatial and Temporal Robustness of Sr/Ca-SST Calibrations in Red Sea Corals:  
772 Evidence for Influence of Mean Annual Temperature on Calibration Slopes.  
773 *Paleoceanogr Paleoclimatology* 33:443–456
- 774 Nobre P, Shukla J (1996) Variations of Sea Surface Temperature , Wind Stress , and  
775 Rainfall over the Tropical Atlantic and South America. *J Clim* 9:
- 776 Omata T, Suzuki A, Kawahata H, Nojima S, Minoshima K, Hata A (2006) Oxygen and  
777 carbon stable isotope systematics in *Porites* coral near its latitudinal limit: The  
778 coral response to low-thermal temperature stress. *Glob Planet Change* 53:137–146
- 779 Pätzold J (1984) Growth rhythms recorded in stable isotopes and density bands in the  
780 reef coral *Porites lobata* (Cebu, Philippines). *Coral Reefs* 3:87–90
- 781 Pereira NS, Sial AN, Frei R, Ullmann C V, Korte C, Kikuchi RKP, Ferreira VP,  
782 Kilbourne KH (2017) The potential of the coral species *Porites astreoides* as a  
783 paleoclimate archive for the Tropical South Atlantic Ocean. *J South Am Earth Sci*  
784 77:276–285
- 785 Pereira NS, Sial AN, Kikuchi RKP, Ferreira VZP, Ullmann C V., Frei R, Cunha AMC  
786 (2015) Coral-based climate records from tropical South Atlantic: 2009/2010 ENSO  
787 event in C and O isotopes from *Porites* corals (Rocas Atoll, Brazil). *An Acad Bras*  
788 *Cienc* 87:1939–1957
- 789 Pereira NS, Sial AN, Kilbourne KH, Liu SC, Shen CC, Ullmann C V., Frei R, Korte C,  
790 Kikuchi RKP, Ferreira VP, Braga BLSS (2018) Carbon stable isotope record in the  
791 coral species *Siderastrea stellata*: A link to the Suess Effect in the tropical South  
792 Atlantic Ocean. *Palaeogeogr Palaeoclimatol Palaeoecol* 497:82–90
- 793 Pereira NS, Voegelin AR, Paulukat C, Sial AN, Ferreira VP (2016) Chromium-isotope  
794 signatures in scleractinian corals from the Rocas Atoll , Tropical South Atlantic.  
795 *Geobiology* 14:54–67
- 796 Pfeiffer M, Reuning L, Zinke J, Garbe-Schönberg D, Leupold M, Dullo W (2019) 20th  
797 Century  $\delta^{18}\text{O}$  Seawater and Salinity Variations Reconstructed From Paired  $\delta^{18}\text{O}$   
798 O and Sr/Ca Measurements of a La Reunion Coral. *Paleoceanogr Paleoclimatology*  
799 34:2183–2200
- 800 Revelle R, Suess HE (1957) Carbon Dioxide Exchange Between Atmosphere and  
801 Ocean and the Question of an Increase of Atmospheric CO<sub>2</sub> during the Past  
802 Decades. *Tellus* 9:18–27
- 803 Reverdin G, Kestenare E, Frankignoul C, Delcroix T (2007) Surface salinity in the  
804 Atlantic Ocean (30°S–50°N). *Prog Oceanogr* 73:311–340
- 805 Roos NC, Pennino MG, Carvalho AR, Longo GO (2019) Drivers of abundance and  
806 biomass of Brazilian parrotfishes. *Mar Ecol Prog Ser* 623:117–130
- 807 Rosenheim BE, Swart PK, Thorrold SR, Eisenhauer A, Willenz P (2005) Salinity



808 change in the subtropical Atlantic: Secular increase and teleconnections to the  
809 North Atlantic Oscillation. *Geophys Res Lett* 32:1–4

810 Santedicola, M.C.R., Kikuchi, R.K.P., Cunha, M.P., Domingues, R.M., Gonçalves,  
811 P.M., 2008. Pilot study on Sr/Ca, Mg/Ca and Ba/Ca ratios in skeletons of  
812 *Mussismilia braziliensis* (Verrill, 1868) as sea surface temperature (SST) proxy in  
813 the coast of Bahia, Eastern Brazil, in: *Oceanografia e Mudanças Globais*. Instituto  
814 Oceanográfico, São Paulo.

815 Santos, C.L.A., Vital, H., Amaro, V.E., Kikuchi, R.K.P., 2007. Mapping of the  
816 submerged reefs in the coast of the Rio Grande do Norte, near Brazil: Macau to  
817 Maracajau. *Rev. Bras. Geofis.* 25, 27–36.

818 Saenger C, Cohen AL, Oppo DW, Hubbard D (2008) Interpreting sea surface  
819 temperature from strontium/calcium ratios in *Montastrea* corals: Link with growth  
820 rate and implications for proxy reconstructions. *Paleoceanography* 23:

821 Schneider T, Bischoff T, Haug GH (2014) Migrations and dynamics of the intertropical  
822 convergence zone. *Nat* 2014 5137516 513:45–53

823 Servain J, Caniaux G, Kouadio YK, McPhaden MJ, Araujo M (2014) Recent climatic  
824 trends in the tropical Atlantic. *Clim Dyn* 43:3071–3089

825 Shen C-C, Wu C-C, Cheng H, Edwards R, Hsieh Y-T, Gallet S, Chang C-C, Li T-Y,  
826 Lam D, Kano A, Hori M, Spöt C (2012) High-precision and high-resolution  
827 carbonate <sup>230</sup>Th dating by MC-ICP-MS with SEM protocols. *Geochim Cosmochim*  
828 *Acta* 99:71–86

829 Shen C-C, Li K-S, Sieh K, Natawidjaja D, Cheng H, Wang X, Edwards RL, Dinh DD,  
830 Hsieh Y-T, Fan T-Y, Meltzner AJ, Taylor FW, Quinn TM, Chiang H-W,  
831 Kilbourne KH (2008) Variation of initial 230 Th / 232 Th and limits of high  
832 precision U–Th dating of shallow-water corals. 72:4201–4223

833 Silva ICBS, Liparini A, Pereira NS, Braga BLSS, Sial AN, Liu S, Shen C, Kikuchi RKP  
834 (2019) Assessing the growth rate of the South Atlantic coral species *Mussismilia*  
835 *hispida* ( Verrill , 1902 ) using carbon and oxygen stable isotopes. *J South Am*  
836 *Earth Sci* 96:1–9

837 Stefano C, Viana PJ, Campos MC, Kuhnert H, Lopes ABM, Cruz FW, Chiessi CM  
838 (2021) Development and characterization of a new in-house reference material for  
839 stable carbon and oxygen isotopes analyses. *J Anal At Spectrom* 36:1125–1134

840 Swart PK (1983) Carbon and Oxygen Isotope Fractionation in Scleractinian Corals: a  
841 Review. *Earth-Science Reviews* 19:51–80

842 Swart PK, Greer L, Rosenheim BE, Moses CS, Waite AJ, Winter A., Dodge RE,  
843 Helmle K (2010) The <sup>13</sup>C Suess effect in scleractinian corals mirror changes in the  
844 anthropogenic CO<sub>2</sub> inventory of the surface oceans. *Geophys Res Lett* 37: L05604.

845 Swart PK, Grottoli a. (2003) Proxy indicators of climate in coral skeletons: a  
846 perspective. *Coral Reefs* 22:313–315

847 Testa V, Bosence DWJ (1999) Physical and biological controls on the formation of  
848 carbonate and siliciclastic bedforms on the north-east Brazilian shelf.  
849 *Sedimentology* 46:279–301

- 850 von Reumont J, Hetzinger S, Garbe-Schönberg D, Manfrino C, Dullo C (2018)  
851 Tracking Interannual- to Multidecadal-Scale Climate Variability in the Atlantic  
852 Warm Pool Using Central Caribbean Coral Data. *Paleoceanogr Paleoclimatology*  
853 33:395–411
- 854 Waliser DE, Gautier C (1993) A Satellite-derived Climatology of the ITCZ. *J Clim*  
855 6:2162–2174
- 856 Watanabe, T., A. Winter, and T. Oba (2001) Seasonal changes in sea surface  
857 temperature and salinity during the little Ice Age in the Caribbean Sea deduced  
858 from Mg/Ca and  $^{18}\text{O}/^{16}\text{O}$  ratios in corals, *Mar. Geol.*, 173, 21– 35,  
859 doi:10.1016/S0025-3227(00)00166-3.
- 860 Watanabe, T., A. Winter, T. Oba, R. Anzai, and H. Ishioroshi (2002) Evaluation of the  
861 fidelity of isotope records as an environmental proxy in the coral *Montastrea*, *Coral*  
862 *Reefs*, 21, 169–178.
- 863 Weber J, Woodhead P (1970) Carbon and oxygen isotope fractionation in the skeletal  
864 carbonate of reef-building corals. *Chemical Geology* 6:93–117
- 865 Weerabaddana MM, DeLong KL, Wagner AJ, Loke DWY, Kilbourne KH, Slowey N,  
866 Hu HM, Shen CC (2021) Insights from barium variability in a *Siderastrea siderea*  
867 coral in the northwestern Gulf of Mexico. *Marine Pollution Bulletin* 173: 112930